Biochimica et Biophysica Acta 1837 (2014) 51–62

Contents lists available at ScienceDirect

Biochimica et Biophysica Acta

journal homepage: www.elsevier.com/locate/bbabio

Availability of the key metabolic substrates dictates the respiratory response of cancer cells to the mitochondrial uncoupling

Alexander V. Zhdanov [a,*], Alicia H.C. Waters [a], Anna V. Golubeva [b], Ruslan I. Dmitriev [a], Dmitri B. Papkovsky [a]

[a] Biochemistry Department, University College Cork, Cavanagh Pharmacy Building, College Road, Cork, Ireland
[b] Alimentary Pharmabiotic Centre, University College Cork, Bioscience Institute, Western Road, Cork, Ireland

ARTICLE INFO

Article history:
Received 4 April 2013
Received in revised form 16 July 2013
Accepted 17 July 2013
Available online 23 July 2013

Keywords:
Cancer cell
Mitochondrial respiration
Glycolysis
Glutaminolysis
Metabolic substrate
Uncoupling

ABSTRACT

Active glycolysis and glutaminolysis provide bioenergetic stability of cancer cells in physiological conditions. Under hypoxia, metabolic and mitochondrial disorders, or pharmacological treatment, a deficit of key metabolic substrates may become life-threatening to cancer cells. We analysed the effects of mitochondrial uncoupling by FCCP on the respiration of cells fed by different combinations of Glc, Gal, Gln and Pyr. In cancer PC12 and HCT116 cells, a large increase in O_2 consumption rate (OCR) upon uncoupling was only seen when Gln was combined with either Glc or Pyr. Inhibition of glutaminolysis with BPTES abolished this effect. Despite the key role of Gln, addition of FCCP inhibited respiration and induced apoptosis in cells supplied with Gln alone or Gal/Gln. For all substrate combinations, amplitude of respiratory responses to FCCP did not correlate with Akt, Erk and AMPK phosphorylation, cellular ATP, and resting OCR, mitochondrial Ca^{2+} or membrane potential. However, we propose that proton motive force could modulate respiratory response to FCCP by regulating mitochondrial transport of Gln and Pyr, which decreases upon mitochondrial depolarisation. As a result, an increase in respiration upon uncoupling is abolished in cells, deprived of Gln or Pyr (Glc). Unlike PC12 or HCT116 cells, mouse embryonic fibroblasts were capable of generating pronounced response to FCCP when deprived of Gln, thus exhibiting lower dependence on glutaminolysis. Overall, the differential regulation of the respiratory response to FCCP by metabolic environment suggests that mitochondrial uncoupling has a potential for substrate-specific inhibition of cell function, and can be explored for selective cancer treatment.

1. Introduction

A role of the mitochondria is that of a 'power plant' of the eukaryotic cell. The electron transport chain (ETC) conducts a cascade of RedOx reactions and generates proton motive force (PMF) which is utilised by F0F1 ATP synthase (complex V) to produce ATP through the oxidative phosphorylation (OxPhos). Being the most effective way of ATP production, OxPhos is tightly regulated. The efficiency of OxPhos, defined by the amount of inorganic phosphate (P*i*) utilised for ATP production per amount of O_2 consumed [1,2], may be affected by a number of factors, including the level of uncoupling between inward mitochondrial H^+ current and ATP synthesis. Indeed, a certain proportion of H^+ is always translocated to inside the matrix bypassing complex V, thus degrading the mitochondrial membrane potential ($\Delta\Psi m$). This so called 'extrinsic' uncoupling can be achieved through the activation of uncoupling proteins, a nonspecific $\Delta\Psi m$-dependent proton leak, general ion symport/antiport and chemical uncouplers [3]. The weak acid protonophore FCCP (carbonyl cyanide 4-(trifluoromethoxy)phenylhydrazone) [4], which provides reversible uncoupling [5] and dissipates PMF in a concentration-dependent manner, [6,7] is commonly used in the experiments with isolated mitochondria and whole cells.

Isolated mitochondria are a simple and well-established model as they are accessible to the metabolic substrates and pharmacological compounds, and independent on complex inter-compartmental transport of biomolecules, cytoplasmic metabolism and ion fluxes [8]. The substrates feeding the Krebs cycle and complexes I–V strongly affect respiration of isolated mitochondria [1,9]. Different combinations of the substrates and co-factors are used for analysis of i) the functional activity of mitochondrial enzymes and contribution of ETC complexes to the total mitochondrial respiration; ii) H^+/O, H^+/ATP and P*i*/O ratios; iii) the state III (and state IV) respiration and respiratory control ratio;

Abbreviations: Akt, protein kinase B (PKB); α-KG, α-ketoglutarate; AMPK, AMP-activated protein kinase; BPTES, bis-2-(5-phenylacetamido-1,2,4-thiadiazol-2-yl)ethyl sulfide; $\Delta\Psi m$, mitochondrial membrane potential; $\Delta\Psi p$, plasma membrane potential; ΔpH, mitochondrial proton gradient; DMEM, Dulbecco's Modified Eagle's medium; DMSO, dimethyl sulphoxide; ECA, extracellular acidification; Erk, mitogen-activated protein kinase (MAPK); ETC, electron transport chain; FBS, fetal bovine serum; FCCP, carbonyl cyanide 4-(trifluoromethoxy)phenylhydrazone; Gal, D-galactose; Glc, D-glucose; Gln, L-glutamine; GLS1, kidney-type glutaminase; Glu, glutamate; GLUT, glucose transporter; GSH, glutathione; HS, horse serum; iO_2, intracellular oxygen; MEFs, mouse embryonic fibroblasts; NGF, nerve growth factor; OCR, oxygen consumption rate; OxPhos, oxidative phosphorylation; PMF, proton motive force; PMPI, plasma membrane potential indicator; Pyr, pyruvate; ROS, reactive oxygen species; RPMI, Roswell Park Memorial Institute; TMRM, tetramethyl rhodamine methyl ester; P*i*, inorganic phosphate; WM, working media

* Corresponding author at: Cavanagh Pharmacy Building, College Road, Cork, Ireland. Tel.: +353 21 4901699; fax: +353 21 4901698.
E-mail address: a.zhdanov@ucc.ie (A.V. Zhdanov).

0005-2728/$ – see front matter © 2013 Elsevier B.V. All rights reserved.
http://dx.doi.org/10.1016/j.bbabio.2013.07.008

and iv) mito-toxicity of the new pharmacological compounds. The O_2 consumption rate (OCR) in isolated mitochondria may be set to different levels by simple addition of the appropriate substrates and drugs affecting respiration. Thus, maximal mitochondrial respiration can be achieved by addition of FCCP to the mitochondria in state III [8].

However, the processes observed in isolated mitochondria may be significantly different from that taking place in intact cells, which have undisturbed cellular networks and environment and represent a more physiologically relevant model for experiments on bioenergetics and metabolism [8]. Mitochondrial respiration in cells is regulated by many factors and the results of uncoupling under physiological conditions are not easy to interpret. Changes in the transport of metabolites and ions across the plasma membrane, a decrease in mitochondrial and increase in cytosolic Ca^{2+}, activation of glycolysis, cytosolic and extracellular acidification, can all strongly affect respiratory responses to FCCP, and even careful optimisation of FCCP concentration for each cell type [8] may not eliminate indirect effects of this drug on cellular respiration and function in general. Thus, dissipation of the mitochondrial ATP flux upon uncoupling can rapidly activate 'non-mitochondrial' metabolic pathways involved in production and preservation of energy (e.g. AMPK) [10]. Therefore, shortages in basic metabolic substrates can contribute to cellular responses to mitochondrial uncoupling and escalate energy stress. Thus, uncoupling becomes life-threatening when glucose (Glc) is replaced with galactose (Gal), as glycolysis can no longer maintain steady ATP levels.

In cancer cells Glc supply becomes essential, since glycolysis produces large amounts of ATP regardless of high availability of O_2 (Warburg effect) [11]. In turn, most of the pyruvate (Pyr), instead of conversion into Acetyl-CoA and utilisation in the Krebs cycle [12], is converted to lactate and extruded from the cell. Some intermediates of glycolysis (e.g. phosphoenolpyruvate) are also re-directed to anabolic reactions producing materials for actively proliferating cancer cells [13–15]. To further accelerate anaplerotic reactions and ATP production, cancer cells addictively utilise glutamine (Gln), and more than half of ATP can be produced through Gln-driven OxPhos [16–19]. As a result, Gln-driven mitochondrial respiration in many cancer cells is active even at high Glc levels [20], and increases further upon replacement of Glc with Gal.

Considering the complexity of the bioenergetic network, one can anticipate that respiration of resting cells supplied with different substrates may not inform correctly on their ability to respond to mitochondrial uncoupling in a classical way, i.e. by prominent and sustained increase in respiration. Here, using rat pheochromocytoma PC12 cell and other cell lines, we studied how the availability and utilisation of major metabolic substrates modulate the respiratory response of cancer cells to mitochondrial uncoupling.

2. Experimental procedures

2.1. Materials

O_2-sensitive probes MitoXpress®-Xtra [21], MitoXpress®-Intra NanO2 [22] and pH-sensitive probe pH-Xtra [23] were from Luxcel Biosciences (Cork, Ireland). Glutaminase inhibitor, BPTES (bis-2-(5-phenylacetamido-1,2,4-thiadiazol-2-yl)ethyl sulfide) [24] was kindly provided by Dr. Takashi Tsukamoto (John Hopkins University, MD). Mitochondrial membrane potential indicator Tetramethyl rhodamine methyl ester (TMRM), Lipofectamine 2000 and Opti-MEM I were from Invitrogen Life Technologies (Carlsbad, CA). Plasma membrane potential indicator (PMPI) [25] was from Molecular Devices (Sunnyvale, CA). ECL Prime Western blotting reagent was from GE Healthcare Life Sciences (Waukesha, WI), pre-made acrylamide gels, running and transfer buffers were from GeneScript (Piscataway, NJ), BCA™ Protein Assay kit was from Thermo Fisher Scientific (Rockford, Ill). The mitochondria-targeted Ca^{2+} biosensor, $_{mito}$Case12 [26] was from Evrogen JSC (Moscow, Russia). CellTiter-Glo® ATP Assay was from Promega (Madison, WI). Mineral oil (type 37) was from Cargille Laboratories (Cedar Grove, NJ). Dulbecco's Modified Eagle's medium (DMEM) and Roswell Park Memorial Institute (RPMI) media, nerve growth factor (NGF), collagen IV, FCCP, D-glucose, D-galactose, L-glutamine, sodium pyruvate and other reagents were from Sigma-Aldrich.

2.2. Composition of the media and experimental conditions

Rat pheochromocytoma PC12 cells, human colon cancer HCT116 cells and mouse embryonic fibroblasts (MEFs) were from American Tissue Culture Collections (ATCC, Manassas, VA). PC12 cells were maintained in suspension in RPMI 1640 medium supplemented with 10 mM HEPES (pH 7.2), 2 mM L-Gln, 10% horse serum (HS), 5% fetal bovine serum (FBS), 100 U/ml penicillin/100 μg/ml streptomycin (P/S) in humidified atmosphere of 5% CO_2 and 95% air at 37 °C. HCT116 and MEFs were maintained in the same conditions in DMEM medium supplemented with HEPES, L-Gln, 10% FBS and P/S.

PC12 cells were differentiated as described previously [26]. Briefly, for experiments with OCR, ECA and iO_2, cells were seeded at 5×10^4 cells/well on 96-well plates (Greiner Bio One, Frickenhausen, Germany) coated with 0.01% collagen IV, and differentiated for 3–5 days in RPMI supplemented with $NaHCO_3$, L-Gln, 1% horse serum, P/S, and 100 ng/ml NGF. For live cell confocal imaging cells were seeded at 2.5×10^4 cells per ~1 cm^2 dish differentiated on glass bottom mini-dishes (MatTek, Ashland, MA) coated with a mixture of collagen IV (0.007%) and poly-D-lysine (0.003%). For protein analysis cells were seeded at 5×10^5 cells per well and differentiated for 5 days on 12-well plates (Corning Life Sciences, NY) coated with collagen IV.

HCT116 and MEFs were seeded in a growing medium at 2.5×10^4 cells/well on 96-well plates (Greiner) coated with 0.01% collagen IV, grown for 2 days prior to analysis.

Working media (WM) were prepared as follows. Powder DMEM (Sigma, cat. No 5030) was reconstituted in deionised water and filter-sterilised. From this plain DMEM, 12 different WM were composed by addition of 100 nM NGF, 10 mM Glc, 10 mM Gal, 2 mM Gln and 1 mM Pyr as shown in Table 1. No serum was added. All WM contained 20 mM HEPES, pH 7.2, except for ECA measurements.

Prior to the experiments, growth or differentiation media were replaced with one of the WM, and the cells were incubated in 5% CO_2 at 37 °C for 2 h. To inhibit glutaminolysis, BPTES (10 μM) was applied to the samples 1 h prior to and kept during the experiments. To uncouple respiration, cells were treated with 1 μM FCCP, optimal for all cell lines, as determined in separate experiment (Supplemental Fig. S1).

2.3. O_2 consumption rate (OCR) assay

Measurement of OCR and iO_2 (see Section 2.5) was performed using a well-established phosphorescence quenching technique [27,28]. Developed for the assessment of O_2 consumption by biological specimens on a conventional fluorescence spectrometer or plate reader [21], a water-soluble phosphorescent O_2-sensitive probe MitoXpress®-Xtra was validated [23,29,30] and used in a number of studies [31–36]. These works demonstrate that the phosphorescence quenching is a

Table 1
Composition of the WM.

Components	WM											
	1	2	3	4	5	6	7	8	9	10	11	12
D-glucose	+	+	+	+								
D-galactose					+	+	+	+				
L-glutamine	+	+			+	+			+	+		
Pyruvate		+	+			+	+			+	+	
NGF[a]	+	+	+	+	+	+	+	+	+	+	+	+

[a] Only for PC12 cells.

simple, non-invasive and versatile quantitative approach which allows for direct, high-throughput, real-time analysis of OCR and provides physiologically relevant data on cell metabolism in a broad range of test samples, from isolated mitochondria [31,37] to small organisms [38,39].

In this study, growth or differentiation media were replaced with WM, and cells were incubated for 2 h (BPTES was added, as required). OCR measurements were conducted in 100 μl of air-equilibrated WM supplemented with 200 nM MitoXpress probe as described [29], in the presence of mitochondrial uncoupler FCCP (1 μM) or solvent (DMSO), which were added to the cells immediately prior to the measurement. Sample wells were quickly sealed with 150 μl of mineral oil pre-warmed to 37 °C and the plate was monitored on a TR-F reader Victor 2 (PerkinElmer Life Sciences) at 37 °C with excitation and emission at 340 and 642 nm, respectively. Each sample well was measured repetitively every 3–5 min over 60–90 min, by taking two intensity readings at delay times of 30 and 70 μs and gate time 100 μs. The intensity signals were converted into phosphorescence lifetime (τ) values as follows: $\tau = (t_2 - t_1) / \ln(F_1 / F_2)$, where F_1 and F_2 are the TR-F intensity signals at delay times t_1 and t_2. Average O_2 levels across the samples were calculated from τ values [30], and then the OCR for each working medium was calculated as O_2 consumed by cells in 1 min per 1 mg of total soluble protein (nmole/min · mg protein) [29,40]. Protein concentrations were measured using BCA™ Protein Assay kit.

2.4. Lactate-specific extracellular acidification assay (L-ECA)

The ECA was measured as described [29]. Firstly, the growth or differentiation media were replaced with 150 μl WM containing 10 mM HEPES and put into CO_2-free conditions at 37 °C for 2 h to release absorbed CO_2. Then the media was replaced with unbuffered WM (without HEPES) and put back into CO_2 free conditions for 1 h (incubation with BPTES was performed as necessary). After that, 100 μl of unbuffered WM containing 1 μM pH-Xtra probe and the stimulants (FCCP or DMSO) were added to experimental wells and the plate was measured on the Victor 2 plate reader at 37 °C for 60–90 min in the TR-F mode with excitation/emission at 340/615 nm. Two TR-F intensity signals were measured at delay times of 100 and 300 μs and a measurement window of 30 μs. The emission lifetime τ was calculated as described for the OCR and converted in pH values [23]. The latter were used to calculate an amount of protons extruded by cells in 1 min per 1 mg of total soluble protein (H^+, mole/min · mg protein). Protein concentrations were measured using BCA™ Protein Assay kit.

2.5. Intracellular O_2 measurement

Developed and validated for the monitoring of O_2 concentration within the cell as large molecules [30,40–43], intracellular phosphorescent O_2 probes were further improved and currently represent cell-penetrating small molecule [44–46] and nano-particle [22,47] based structures. The probes allow for precise quantitative real-time monitoring of cell oxygenation levels at different conditions [48,49], and of rapid transient changes in respiration upon cell treatment [26,42]. Described in detail and validated in [22,47], MitoXpress®-Intra NanO2 probe represents a non-toxic convenient sensor, working with high throughput, reproducibility and efficiency in plate reader and fluorescence microscope platforms, as reviewed in [27,28]. Most recently, the probe was effectively applied for hypoxia research [34,48].

In this study, cells were incubated in the medium containing 10 μg/ml NanO2 probe for 18–24 h at 37 °C [22], then washed with DMEM supplemented with 1% HS (supplied with NGF for PC12 cells) and with WM (150 μl). Then WM were replaced by a fresh aliquot (200 μl) and the cells were incubated at 37 °C (BPTES was added when needed). Two hours later WM were replaced with a fresh aliquot (200 μl), and plate was transferred to Victor 2 reader TR-F reader placed at 20.9% O_2 or in a hypoxia chamber (Coy Laboratory Products, Grass Lake, MI) pre-set to 4.5% O_2. Monitoring of iO_2 was performed similarly to OCR measurements at 37 °C with 340 nm excitation and 642 nm emission spectra. The O_2 concentrations and cell deoxygenation rates were calculated as described [22].

Briefly, the plate was incubated in the reader for 10 min and then monitored for ~20 min to achieve steady-state oxygenation of resting cells, then the plate was quickly withdrawn from the reader, 1 μM FCCP was added to the cells (20 μl of 10× stock solution) and monitoring was resumed for further 30 min.

2.6. Monitoring of ΔΨp, ΔΨm and mitochondrial Ca^{2+}

PC12 cell at were seeded at 2.5×10^4 cells per cm^2 and differentiated for 4–5 days with NGF on glass bottom mini-dishes (MatTek) coated with a mixture of collagen IV (0.007%) and poly-D-lysine (0.003%). Transfection with mitoCase12 plasmid was carried out using Lipofectamine 2000 and Opti-MEM I medium (Invitrogen), as per manufacturer procedure. Loading with fluorescent sensors TMRM (20 nM) and PMPI (1:200) was performed for 30 min in Opti-MEM I medium with Ca^{2+} concentration adjusted to 2 mM. During the measurements, TMRM and PMPI were maintained in solution at 20 nM and 1:1000 dilution, respectively.

Confocal live cell fluorescence imaging was conducted on Olympus FV1000 confocal laser scanning microscope with controlled CO_2, humidity and temperature. The mitoCase12 probe was excited at 488 nm (2.5–5% of maximal laser power) with emission collected at 500–540 nm. TMRM and PMPI probes were excited at 543 nm (2.5% and 1%, respectively) collecting emission with a 555–600 nm filter. The probes were mostly used individually, although in some experiments TMRM and mitoCase12 were used simultaneously. Since mitoCase12 can decrease the TMRM staining (when expressed at very high levels), only the cells with unaffected TMRM signal were selected for analysis. Acquisition of each spectral signal was done in sequential laser mode with emission gates adjusted to avoid overlaps.

ΔΨm and ΔΨp were depolarised with 1 mM FCCP and 100 mM KCl [42], respectively. In all experiments the differential interference contrast and fluorescence images were collected kinetically with a 60× oil immersion objective in two planes using 0.5 μm step and 20–30 s intervals. The resulting z-stacked images were analysed using FV1000 Viewer software (Olympus), Excel, Adobe Photoshop and Illustrator.

2.7. Protein isolation and Western blot analysis

The cells were differentiated on 12-well plate and pre-incubated for 2 h in different WM. The media were replaced with the fresh aliquots (2 ml per well), and the cells were incubated at 37 °C for 4 h in 6 WM (see Results section) with or without 1 μM FCCP. Whole cell lysate proteins were prepared as described [49]. Briefly, cells were washed twice with PBS containing phosphatase inhibitors and lysed for 15 min on ice with lysis buffer, containing 150 mM NaCl, 1 mM EDTA, 1% IGEPAL® CA-630, 50 mM HEPES (pH = 7.5) and protease inhibitors (Roche, Ireland). After lysate clarification by centrifugation for 10 min at 16,000 *g* and 4 °C, protein concentrations were measured using BCA™ Protein Assay kit and normalised. Proteins were separated by 8% and 4–20% polyacrylamide gel electrophoresis (GenScript, NJ and Bio-Rad, CA), transferred onto a 0.2 μm Immobilon™-P PVDF membrane (Sigma) using wet mini-transfer system Hoefer™ TE 22 (Hoefer, CA) and probed with antibodies against PARP (Poly(ADP-ribose) polymerase), LC3A/B, phospho-p44/42 Erk, phospho-AMPKα, phospho-Akt, phospho-mTOR (all from Cell Signalling, catalogue numbers, respectively: 9542, 9101, 4108, 2535, 4060, 2971) and α-tubulin (Sigma, T5168). Incubations with antibodies were performed in 5% fat-free milk or 5% BSA in TBST overnight at 4 °C (primary) and 2 h at room temperature (secondary). Blots were visualised and analysed with HRP-conjugated secondary antibodies (Sigma) and ECL prime reagents using the LAS-3000 Imager (FujiFilm, Japan) and Image Reader LAS-3000 2.2 software.

Quantitative image analysis was performed with ImageJ program using α-tubulin signals for normalisation. Images were processed with Picasa, Photoshop, and Illustrator programs.

To normalise the results of metabolic assays for total protein content in different samples, proteins were prepared as above and measured using BCA™ Protein Assay kit.

2.8. ATP measurement

Analysis of total cellular ATP was performed using CellTiter-Glo® assay, following the manufacturer's protocol. Briefly, cells were seeded and treated as described in Sections 2.2 and 3 and were lysed with CellTiterGlo® reagent. After intensive shaking for 2 min, the samples were transferred into wells of white 96-well plates (Greiner Bio One) and read on a Victor 2 (PerkinElmer) plate reader under standard luminescence settings.

2.9. Statistics

Statistical analysis was performed using the results of 3–6 independent experiments. Confidence levels of 0.01 and 0.001 were deemed as statistically significant. To ensure data accuracy and fidelity, the majority of the experiments were performed in 3–8 replicates.

The levels of OCR, ECA, iO_2 and ATP were normalised to the total protein content in the samples. ATP levels were normalised to ATP content in untreated cells in Glc/Pyr/Gln medium, which was defined as 1 a.u. Fluorescence intensities on the confocal images (PMPI, TMRM, mitoCase12) were examined in kinetic mode analysing 5–20 cells in 3 independent experiments. The differences between the mean values were evaluated using two-tailed Student t-test (equality of variances in the samples was first estimated using Levene's test). The differences in iO_2, TMRM, mitoCa^{2+} (in Δ%) were evaluated using Mann–Whitney U-test.

3. Results

3.1. Effect of metabolic substrate composition on the respiratory response to FCCP

A highly metabolically active cell line with equally well developed glycolytic and mitochondrial ATP fluxes [29], PC12 cells are commonly used for studies on bioenergetics of cancer and neuronal cells [50–52]. Mitochondrial uncoupling with FCCP continuously increases respiration, and activates glycolysis in PC12 cells supplied with Glc, Pyr and Gln [42]. Here, we pre-incubated differentiated PC12 cells in 12 different working media (WM, Table 1) for 2 h to achieve metabolic 'adaptation', and then treated them with 1 μM FCCP.

Cell oxygenation is inversely related to their respiratory activity, and changes in intracellular O_2 (iO_2) report on the magnitude of the respiratory response to stimulation [29,30]. We found that the highest basal OCR was provided by Gln combined with Pyr (with or without Gal). Consuming O_2 at a rate of ~5 nM/min per 1 mg of total soluble protein, the cell monolayer maintained iO_2 at 95 ± 5 μM (Fig. 1A). Cells utilising Gln plus Glc/Pyr or Gal also exhibited high respiratory activity (over 4 nM/min per 1 mg of protein) and were strongly deoxygenated. The other WM were scored according to cells respiration as follows: Gln > Pyr, Pyr/Gal, Glc/Gln ≫ Gal, no substrates. In WM containing Pyr or Gln, addition of Glc decreased respiration.

Upon addition of FCCP we observed four types of respiratory responses, classified according to the changes in cell oxygenation $\Delta iO_2 = iO_{2(t)} - iO_{2(0)}$, where $iO_{2(0)}$ and $iO_{2(t)}$ are the O_2 concentrations in the cell monolayer before and at any time point after FCCP addition, respectively. Changes in iO_2 agreed with the data on OCR (Table 2), calculated for the initial linear phase of the experiments (Supplemental Fig. S2).

The first type was characteristic for the cells supplied with Gln combined with either Glc or Pyr (Fig. 1B, C). Cell deoxygenation was deep and continuous (over 1 h), suggesting steady increase in mitochondrial respiration. Equally large ΔiO_2 were observed in the cells exhibiting high (Gal/Pyr/Gln, Pyr/Gln) and moderate (Glc/Gln, Glc/Pyr/Gln) OCR at rest.

The second type, a significant inhibition of respiration characterised by progressive reoxygenation, was seen in the cells supplied with Pyr or Gln (with or without Gal). Initial minor transient decrease in iO_2 could be observed. A decrease in respiration in the cells supplied with Gln or Gal/Gln was particularly surprising, since 'resting' OCR in these cells was high (Fig. 1A).

The third type, a moderate transient drop in iO_2, was observed in the cells supplied with Glc/Pyr. After partial restoration, iO_2 remained slightly decreased for up to 1 h, indicating that OCR was continuously increased.

The forth type, no changes or slow progressive increase in iO_2, was observed in the cells supplied with Glc and in the low-respiring cells deprived of all substrates or supplied with Gal.

Strong decrease in respiration observed in the cells supplied with Gal/Gln or Gln suggested possible inhibition of cellular function and cell death. Using microscopy and Western blotting analysis, we found that treatment with FCCP for 4 h caused partial detachment of cell from collagen-coated surface and active apoptosis, as indicated by PARP degradation [53] (Fig. 1D). LC3 I/II ratio [54] was decreased in all cells treated with FCCP, pointing to an activation of autophagy.

3.2. Metabolic substrates regulate interplay between respiration and other bioenergetic parameters and pathways upon uncoupling with FCCP

To explain the striking differences in the respiratory responses to FCCP, we analysed effects of metabolic substrates on a number of bioenergetic parameters, such as ATP levels, glycolytic activity, ΔΨm and mitochondrial Ca^{2+}.

We did not find significant differences in resting ATP levels, except for the cells deprived of all substrates or supplied with Gal alone (Fig. 2A). Only a minor decrease in ATP levels was observed within 60 min after the addition of FCCP to the cells supplemented with Glc in any combination (Fig. 2B). In contrast, without glycolytic ATP flux, cellular ATP decreased dramatically within 10 min after the addition of FCCP. Detectable by L-ECA analysis only in the cells supplied with Glc, glycolytic activity was inversely related to OCR (Figs. 2C and 1A). Upon uncoupling, L-ECA markedly increased in the samples containing Glc/Gln or Glc/Pyr/Gln, which produced a strong continuous respiratory response to FCCP (Fig. 1B, C).

No correlation between ATP levels and ΔiO_2 was seen upon uncoupling (10 min: $r = 0.13$, $p = 0.28$; 60 min: $r = 0.08$, $p = 0.46$), suggesting that ATP does not regulate the respiratory response to FCCP. Indeed, equally strong responses were observed in the cells with the highest (Glc/Gln) and the lowest (Pyr/Gln) ATP levels, while in the presence of Glc (high ATP) or Gal alone (low ATP) the responses were very low.

Likewise, changes in respiration did not depend on ΔΨm and mitochondrial Ca^{2+} levels, which were probed by TMRM and mitoCase12 [26] staining, respectively. Using confocal live cell imaging, we observed similar levels in ΔΨm polarisation in all resting cells, except for the cells supplied with only Gal or deprived of all substrates (Fig. 3A). Within 2–5 min after FCCP addition, ΔΨm and mitochondrial Ca^{2+} drastically decreased in a similar manner (Fig. 3B and C, Supplemental Table S1). Plasma membrane potential (ΔΨp), probed by PMPI, was not affected by FCCP. It should be noted, that in cells deprived of substrates, the ΔΨp was substantially depolarised at rest (Supplemental Fig. S3).

Substantial changes in iO_2 and perturbed ATP and ion turnover could affect major pathways involved in hypoxia signalling and energy maintenance. We performed Western blotting analysis of AMPKα and Erk1/2 (p44/p42) phosphorylation in the samples treated with FCCP for 4 h (Fig. 3D) and found that Erk pathway was strongly affected by mitochondrial uncoupling. The levels of p42 Erk (Tyr204)/p44 Erk (Thr202), Akt (Ser473) and mTOR (Ser2448) phosphorylation were

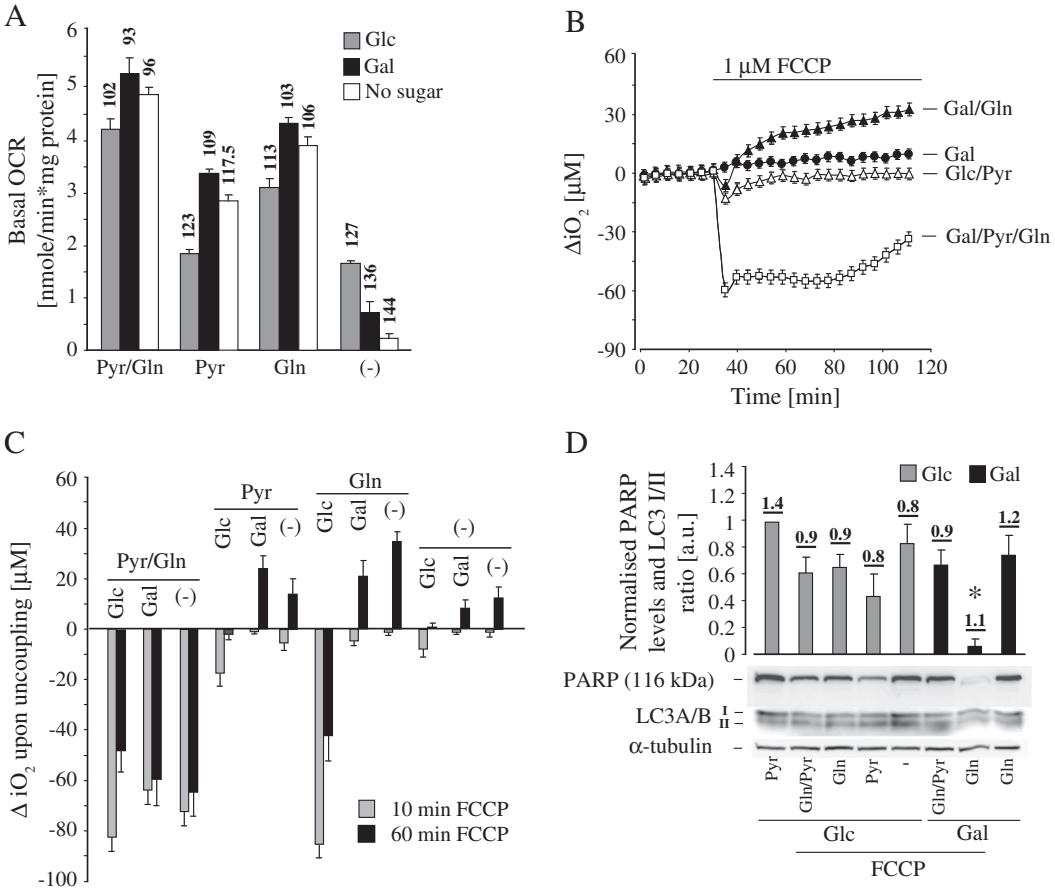

Fig. 1. Substrate composition orchestrates respiratory responses of PC12 cells to mitochondrial uncoupling. A. The levels of OCR (bars) and oxygenation of the cells at rest (shown as numbers above the bars). B. Representative ΔiO_2 (in μM) profiles demonstrate four scenarios of the respiratory response to FCCP treatment: i) rapid decrease in iO_2 followed by continuous deep cell deoxygenation (Gal/Pyr/Gln); ii) inhibition of respiration and cell reoxygenation (Gal/Gln); iii) rapid transient decrease in iO_2 followed by steady minor cell deoxygenation (Glc/Pyr); iv) no changes or slow progressive cell re-oxygenation (Gal). For each medium ΔiO_2 in resting cells was assumed as 0 μM. C. ΔiO_2 within 10 min and 60 min of FCCP treatment: steady deoxygenation is observed only in cells, supplied with Gln in combination with either Pyr or Glc. If the medium does not contain Glc, the lack of either Pyr or Gln leads to progressive cell reoxygenation, suggesting substantial inhibition of respiration. D. Western blotting analysis of LC3A/B I/II ratio (numbers above the bars) and PARP degradation demonstrate that FCCP treatment for 4 h moderately increases autophagy in all samples and strongly activates apoptosis in cells supplied with Gal/Gln. Error bars represent SD, asterisk in (D) shows significant decrease in PARP levels in cells supplied with Gal/Gln ($p < 0.001$); $n = 6$ (A–C) and 3 (D).

significantly decreased in the cells supplied with Glc (particularly with Glc/Pyr/Gln and Glc/Gln), and increased in the cells fed with Gal/Pyr/Gln (except for m-TOR). AMPKα phosphorylation in all samples treated with FCCP was slightly lower than in non-treated controls. In the cells supplied with Gal/Gln, phosphorylation of the aforementioned proteins was not observed.

3.3. Role of glutaminolysis in the respiratory response to FCCP

In agreement with a dominating role of Gln in bioenergetics of cancer cells [18,19], we observed the most prominent respiratory response to FCCP only in the cells supplied with Gln. To further address the role of glutaminolysis in the cellular response to uncoupling, we used BPTES, a specific inhibitor of kidney-type glutaminase (GLS1). An inhibition of GLS1 was achieved by incubation of the cells with 10 μM BPTES for 1 h prior to and during the experiments. This concentration was shown to inhibit glutaminolysis by 80% in solubilised extracts of rat kidney liver mitochondria [24].

Table 2
Changes in OCR upon mitochondrial uncoupling with FCCP.

WM	No addition	Pyr	Gln	Pyr/Gln
Glc	5	11	51	48
Gal	−63[a]	−16	−25	27
No sugar	N/A[a]	−59	−96	23

Data shown in Δ%.
[a] OCR at rest is very low.

BPTES was seen to have no major effect on cellular ATP in resting cells (Table 3), demonstrating that residual GLS1 activity maintained sufficient energy levels in the cells deprived of Glc. Upon uncoupling, GLS1 inhibition leads to a faster decrease in ATP in these cells (see also Fig. 2B), highlighting the importance of glutaminolysis for energy balance.

In the WM containing Gln, treatment with BPTES only slightly affected 'resting' levels of OCR and iO_2 (Fig. 4A and C, Table 4). Upon uncoupling the effect of BPTES was seen clearly: the response of the first type was almost completely abolished (see also Fig. 1). Moreover, in the cells supplied with Gal/Pyr/Gln or Pyr/Gln (Fig. 4B, C), reoxygenation was observed, which was similar to the second type response in WM containing Gal/Pyr or Pyr, respectively (Fig. 1C). In the media without Gln, respiration was not affected by BPTES treatment, demonstrating high specificity of the drug.

Analysing the effect of GLS1 inhibition on the rate of glycolysis in the media supplemented with Glc, we found that treatment with BPTES increased L-ECA rate in resting cells supplied with Glc/Gln/Pyr and Glc/Gln (2.6-fold and 1.5-fold, respectively), suggesting significant activation of glycolysis (Fig. 4D). L-ECA rate in uncoupled cells was almost unaffected.

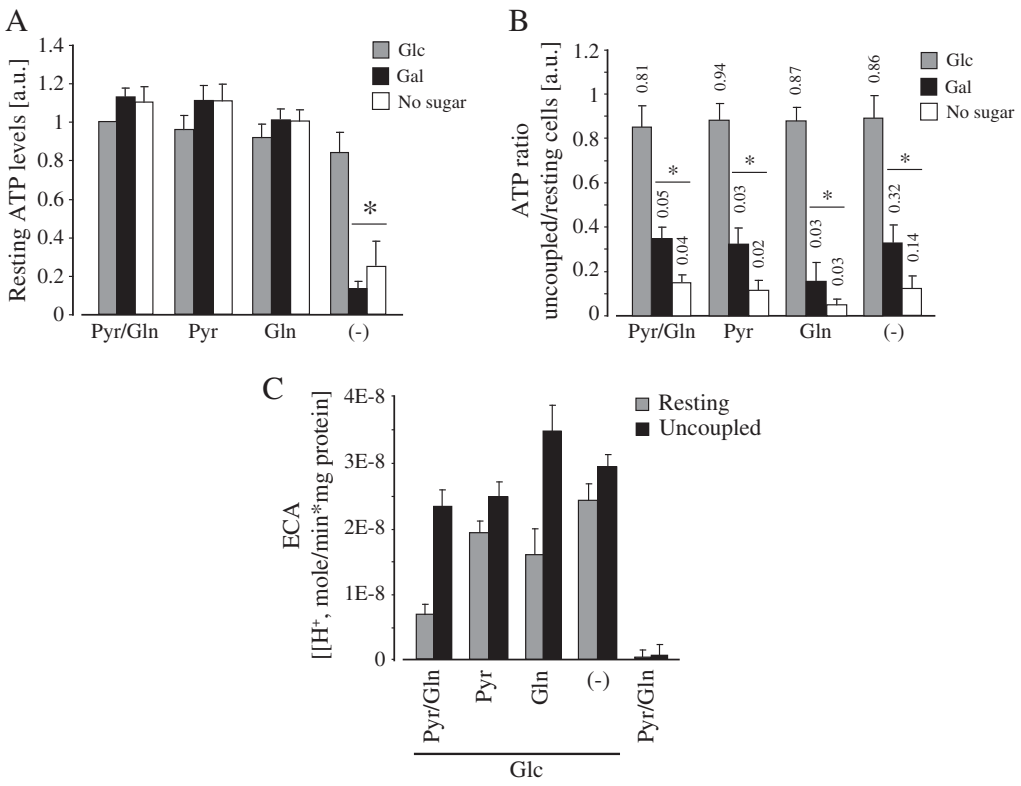

Fig. 2. Substrate composition modulates the effect of FCCP on ATP levels and glycolytic activity in PC12 cells. A. Basal levels of ATP in the cells supplied with the different substrates (3 h time-point). B. Treatment with FCCP strongly affects cellular ATP in the cells deprived of Glc. Data are presented as a ratio between ATP levels in uncoupled and resting cells. Bars and numbers above the bars correspond to 10 and 60 min time-points after FCCP addition, respectively. In the cells supplied with no substrates or Gal alone, relative changes in ATP levels are smaller, because the resting ATP levels are strongly decreased (A). C. Glycolytic activity of the cells measured using L-ECA analysis. Basal L-ECA is inversely related to OCR. Treatment with FCCP substantially increases glycolysis in the cells exhibiting the highest respiratory responses (Glc in combination with Gln on Pyr/Gln). Asterisks indicate significant difference from the value observed in the cells supplied with Glc/Pyr/Gln. Error bars represent SD, $n = 4$.

3.4. Cell specificity of the responses to FCCP

In human colon cancer HCT116 cells, a common model for studies on cancer cell metabolism, we anticipated similar to PC12, Gln-dependent respiratory responses to FCCP. In contrary, in non-cancer MEFs, immortalised with SV40 large T antigen [55,56], glutaminolysis can be strongly activated by Myc oncogene [16], suggesting relatively low rate of Gln utilisation in resting MEFs. Based on these observations we expected a specific pattern of the response to uncoupling in MEFs, distinct from that observed in cancer cells.

Indeed, HCT116 cells exhibited high overall resemblance with PC12 cells in OCR and oxygenation levels at rest and upon uncoupling (Fig. 5). The most pronounced decrease in iO_2 upon FCCP treatment was observed in the cells supplied with Gln with either Pyr or Glc (with or without Gal), however in the presence of Glc this effect was less prominent than in PC12 cells (Fig. 5A, C). Akin to PC12 cells, HCT116 cells could not withstand uncoupling when supplied with Gln or Gal/Gln; although iO_2 levels were low at rest, they noticeably increased upon addition of FCCP, suggesting a decrease in OCR. Treatment with BPTES caused a large reduction of the responses in all cells supplied with Gln and normally strongly increasing respiration upon uncoupling. However, HCT116 exhibited lower sensitivity to BPTES than PC12 cells.

In MEFs, the response to uncoupling was generally more rapid and transient (Fig. 5B, C). Although Gln remained important for generating pronounced responses to FCCP, they were quite specific and could be classified as: 1) type one—rapid increase in respiration, followed by partial or complete restoration of 'resting' iO_2 levels (Gln in all combinations with Glc and Pyr, as well as Glc/Pyr); 2) type two—decrease in respiration and cell reoxygenation (no substrates, Gln and Pyr alone or in combination with Gal); and 3) type three—no significant changes in respiration and iO_2 (Glc or Gal alone). Unlike PC12 and HCT116 cells, the most prominent response to FCCP was observed in MEFs supplied with Glc/Pyr/Gln (down to 20 μM iO_2), and GLS1 inhibition only partially decreased the response to uncoupling. Moreover, MEFs deprived of Gln and supplied with Glc/Pyr were capable of generating continuous positive response to FCCP (Fig. 5C).

4. Discussion

The contribution of a metabolic substrate to mitochondrial respiration is determined by its transport across cell membranes and efficiency of utilisation by corresponding pathway(s).

Cells generate ATP mainly through glycolysis and OxPhos. The absence of Glc can be compensated by increased OxPhos flux and mitochondrial respiration, provided that Pyr and Gln are available. Gln is a key metabolite required for energy production and anaplerotic reactions in cancer cells [16]. In many cell types it is efficiently utilised through glutaminolysis, giving rise to over 50% of cellular ATP and maintaining respiration at high levels [20].

In agreement with this, we observed highest OCRs in the cells supplied with Gln and Gln/Pyr (Fig. 1A). In all media containing Pyr or Gln, respiration was decreased in the presence of Glc because ATP production was partially shifted from OxPhos to glycolysis. Without Pyr or Gln added to the medium, respiration was supported by Glc oxidation.

Sustained H^+ transport across the inner mitochondrial membrane by FCCP rapidly and sustainably dissipates the $\Delta\Psi m$ and ΔpH [5]. In these conditions ATP is no longer produced by the mitochondria; instead, mitochondrial complex V consumes ATP working in reversed mode on the restoration of ΔpH. As a result, glycolysis must be activated to compensate for the loss of OxPhos flux and to supply complex V with ATP.

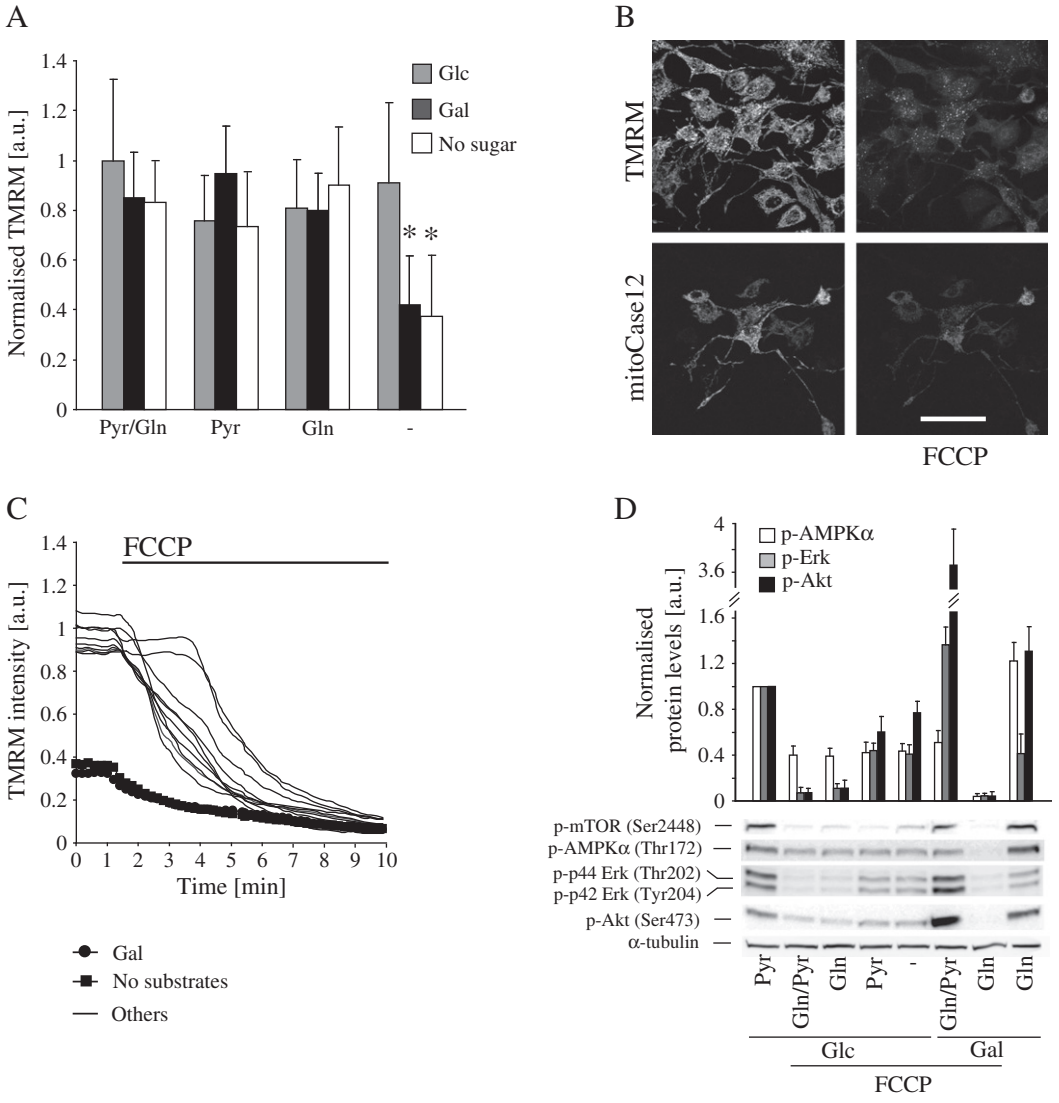

Fig. 3. Effect of substrate composition on the ΔΨm depolarisation and protein phosphorylation upon mitochondrial uncoupling. A. Quantitative analysis of TMRM intensities at rest shows a significant decrease in the ΔΨm only in the cells supplied with no metabolic substrates or Gal. B. Representative effect of FCCP treatment on the ΔΨm and mitochondrial Ca^{2+}, stained with TMRM and mitoCase12 probes (respectively). Right panel demonstrates probe intensities at 8 min after FCCP addition. C. The profiles of ΔΨm depolarisation upon treatment of the cells with FCCP. Asterisks indicate significant difference from the cells supplied with Glc/Pyr/Gln. D. Western blotting analysis of p42 Erk (Tyr204), p44 Erk (Thr202), Akt (Ser473), AMPKα (Thr172) and mTOR (Ser2448) phosphorylation upon FCCP treatment (for 4 h). Bar chart demonstrates quantitatively the substrate-dependent difference in phosphorylation of Erk (combined p42 and p44), Akt and AMPKα. In all cases the levels of protein phosphorylation were normalised to the total protein contents, which remained almost unchanged (not shown). Bar in (B) represents 50 μm. Error bars demonstrate SD of the probe intensities within a cell population (60–80 cells in total); $n = 4$.

Analysis of total ATP revealed striking differences in the levels of energy stress experienced by the cells upon uncoupling. When deprived of Glc, PC12 cells rapidly lost ATP (Fig. 2), while in the presence of Glc ATP levels remained almost unchanged. This although expected, demonstrates that 'respiratory performance' of uncoupled mitochondria, surprisingly, does not depend on cellular ATP, which is often used as a marker of cell viability. Indeed, no correlation was found between ATP levels and the magnitude of the respiratory responses to FCCP, and even after dramatic decreases in ATP (by up to 85% within 10 min) cells supplied with Gln plus Pyr were capable of maintaining a high respiration rate for more than 1 h.

The most pronounced responses were observed in WM containing Gln combined with Glc or Pyr, which agrees with 'Gln addiction' of cancer cells (Figs. 1, 4, 5, Supplemental Fig. S2). However, considering the dominant role of glutaminolysis in cancer metabolism, a decrease in respiration upon uncoupling of the cells supplied with Gln or Gal/Gln

Table 3
Effect of GLS1 inhibition on ATP levels in the cells at rest and upon uncoupling.

WM and treatment	Glc/Pyr/Gln	Glc/Pyr	Glc/Gln	Glc	Gal/Pyr/Gln	Gal/Gln	Pyr/Gln	Gln
Resting	0.99	1.04	1.04	1.02	1.06	0.89	0.95	0.88
Uncoupled	1.07	1.11	1.04	1.14	0.78	0.56	0.37	0.43

Data are shown as BPTES(+)/BPTES(−) ratio in arbitrary units (a.u.).

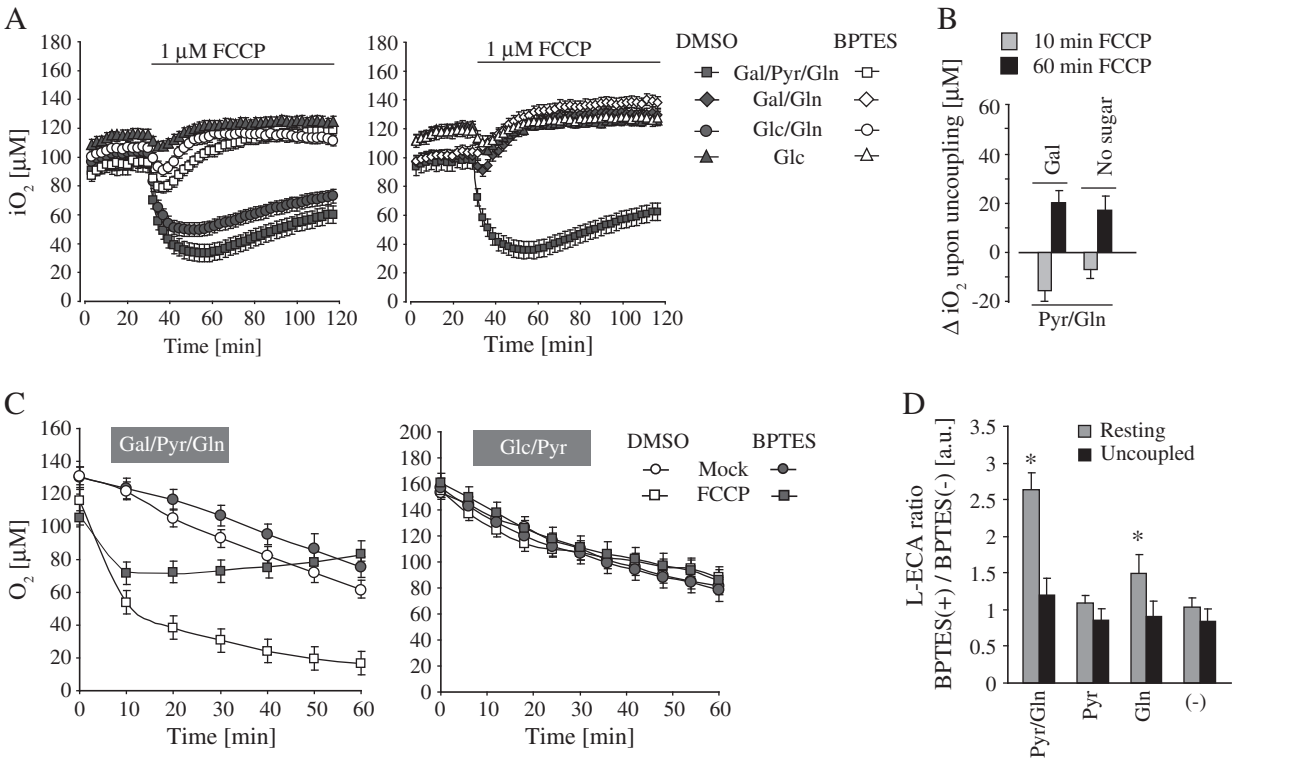

Fig. 4. Effect of GLS1 inhibition on the respiratory response to mitochondrial uncoupling in PC12 cells. A. Representative iO_2 profiles demonstrate that the most intense responses to FCCP (cells supplied with Gal/Pyr/Gln and Glc/Gln) are largely suppressed upon inhibition of GLS1 with 10 μM BPTES. B. Changes in iO_2 (ΔO_2) within 10 min and 60 min of FCCP treatment: upon inhibition of glutaminolysis, iO_2 continuously increases in the uncoupled cells supplied with Pyr/Gln (with or without Gal), suggesting substantial inhibition of respiration. C. For all cells supplied with Gln, OCR profiles reveal that BPTES strongly inhibits responses to FCCP, but not resting cellular respiration (left panel). For the cells deprived of Gln, no effect of BPTES is seen (right panel). D. Effect of GLS1 inhibition on L-ECA rate in resting and uncoupled cells supplied with Glc. Error bars represent SD, $n = 4$.

was unexpected. Although 'resting' O_2 consumption rate in these cells is very high, FCCP not only inhibits mitochondrial function, but also induces apoptosis (Fig. 1D).

To explain this phenomenon, we reviewed Gln transport and utilisation pathways. As shown schematically (Supplemental Fig. S4), Gln is transported into the cytosol via a Gln transporter SN1 and amino acid transporters ASCT1/ASCT2, all of which involve Na^{2+} co-transport and may potentially be affected by the ΔΨp depolarisation. Since upon uncoupling no effect on the ΔΨp was seen, non-specific effects of FCCP on Gln transport across plasma membrane can be ruled out (Supplemental Fig. S3).

Mitochondrial transport of Gln and its derivatives is versatile. Since differentiated PC12 cells exhibit similarities with neuronal cells, transport via mitochondrial glutamine carrier, typical for brain tissues [57] is particularly relevant (Fig. 6). Although electroneutral, Gln uptake by the mitochondria in neurons depends on the ΔpH, and therefore can be suppressed by inhibiting (rotenone) and uncoupling (FCCP) the mitochondria [58]. Gln can also be converted by cytosolic glutaminase into glutamate (Glu), which then enters the mitochondria through either Glu carriers or Glu–Asp antiporters, the latter are a part of the malate–aspartate (Mal–Asp) shuttle [59]. Shuttle activity is directed to the translocation of the reducing equivalents (NADH) from the cytosol, where they are produced mainly through glycolysis and Pyr decarboxylation, into the mitochondria across the mitochondrial membrane, which is impermeable for NADH. In Glc/Pyr-deprived cells, transport of the cytosolic Gln derivatives through the Mal–Asp shuttle is inhibited due to a deficiency in cytosolic NADH. Moreover, Glu–Asp antiporters are electrogenic and require electrochemical potential across the mitochondrial membrane [60], which is perturbed in uncoupled cells. In turn, Glu carriers [61] translocate Glu into the mitochondrial matrix in a symport with H^+, and therefore this pathway is also inhibited upon dissipation of ΔpH with FCCP. Taken together, without Glc and Pyr supply, when the Mal–Asp shuttle activity is decreased, uncoupling can partially inactivate mitochondrial Gln and Glu carriers and decrease respiration, as demonstrated in our experiments.

FCCP can also affect the pathways recruiting Glc and Pyr in OxPhos. Transported into the cell through GLUT-1 and GLUT-4, Glc is converted to Pyr, which can be also delivered into the cell via the H^+-linked monocarboxylate transporter (MCT). Since in our experiments FCCP did not affect the ΔΨp, transport of Glc and Pyr across the plasma membrane should not change much. From the cytosol Pyr enters the mitochondria by means of H^+-coupled symport through the mitochondrial pyruvate carriers (MPC) (Fig. 6) [62,63], and is converted to acetyl-CoA and α-ketoglutarate (α-KG) by pyruvate dehydrogenase and pyruvate carboxylase, respectively. The rate of Pyr transport into the mitochondria through MPC is PMF-dependent and decreases upon its

Table 4
Effect of GLS1 inhibition on OCR in the cells at rest and upon uncoupling.

WM and treatment	Glc/Gln/Pyr	Glc/Gln	Glc/Pyr	Glc	Gal/Gln/Pyr	Gal/Gln	Gal/Pyr	Gal	Gln/Pyr	Gln	Pyr	–
Resting	0.97	0.96	1	0.88	0.93	0.66	1.04	0.93	0.95	0.86	1.09	N/A
Uncoupled	0.56	0.22	1	1	0.12	0.47	0.97	0.90	0.11	0.2	0.94	N/A

Data are shown as BPTES(+)/BPTES(−) ratio in arbitrary units (a.u.).

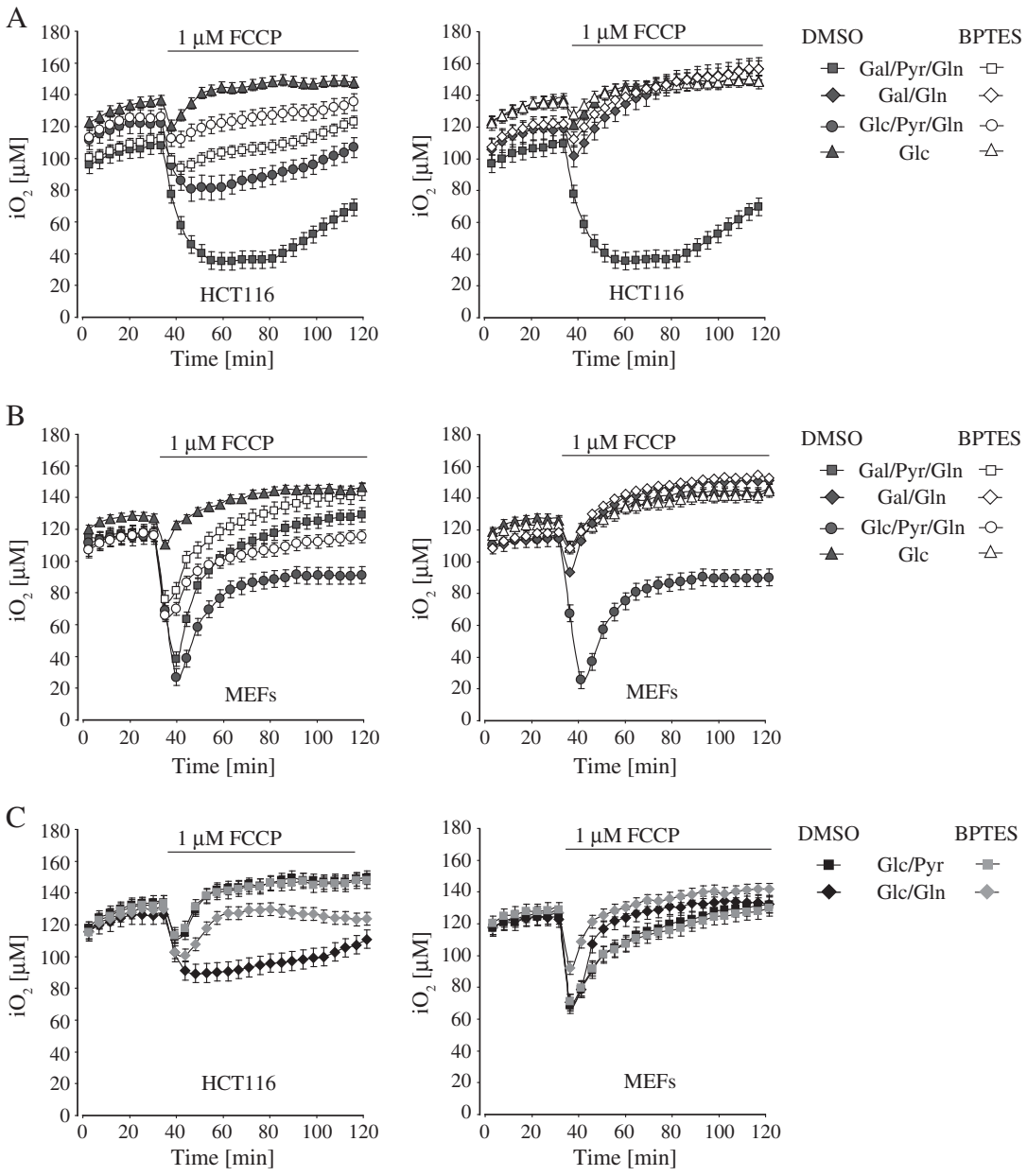

Fig. 5. Differential regulation of the respiratory responses to FCCP in HCT116 and MEFs by metabolic substrates availability and inhibition of glutaminolysis. A. In HCT116 cells the iO_2 profiles demonstrate high resemblance to that observed in PC12 (four types of the response to FCCP). The most intense responses observed in the cells supplied with Gal/Pyr/Gln and Glc/Gln, are decreased upon inhibition of GLS1 with 10 μM BPTES. B. In MEFs the dynamics of the responses are significantly different: rapid deoxygenation of the cells supplied with Gln in combinations with Glc or Pyr is followed by partial reoxygenation and stabilisation of iO_2 levels. In the cells supplied with Gal/Gln or Glc, the levels of iO_2 progressively decreased or remained almost unchanged. Treatment with BPTES has a significantly smaller effect on the respiratory response, than in PC12 or HCT116 cells. C. In contrast to HCT116 cells, MEFs are capable of producing a noticeable respiratory response to uncoupling when supplied with Glc/Pyr. For a mock control for BPTES, cells were treated with DMSO. Error bars represent SD, $n = 4$.

dissipation [63], which occurs in all the media upon uncoupling (Fig. 3). This can explain why no significant increase in mitochondrial respiration is observed upon addition of FCCP to the cells supplied only with Glc, Pyr or Glc/Pyr. A detailed quantitative comparative analysis of activity of the transporters involved in Gln and Pyr uptake in intact and uncoupled mitochondria would be very interesting.

However, other factors can also contribute to the 'non-classical' respiratory responses to FCCP in the cells supplied with Glc and deprived of Gln [64–66]. It has been shown that in the presence of Gln, Glc transport can be activated by α-KG (produced through glutaminolysis and the Krebs cycle), which causes transcriptional repression of the thioredoxin-interacting protein (TXNIP) through interaction with MondoA protein. Upon Gln deprivation or inhibition of glutaminolysis, the levels of α-KG in the cells are decreased, and therefore MondoA activates TXNIP expression, leading to a decrease in Glc uptake. The mechanism is based on Glc-dependent nuclear accumulation of MondoA and formation of MondoA:MIX (Max-like protein X) complex, which is known as transcriptional activator of TXNIP.

Additionally, a dramatic decrease in mitochondrial Ca^{2+} upon uncoupling (Fig. 3) can lead to the partial inhibition of the Krebs cycle enzymes pyruvate, isocitrate and α-ketoglutarate dehydrogenases [67], thus decreasing the amount of the reducing equivalents fed into the electron transport chain and ultimately down-regulating ATP production. Cell toxicity of FCCP, related to its ability to interact with mitochondrial thiols and aminothiols (cysteine, glutathione (GSH)) [68] and to reduce expression of genes associated with cell stress protection [69] can also be differently modulated by metabolic substrates. Similarly, substrate composition may be an important factor regulating FCCP-

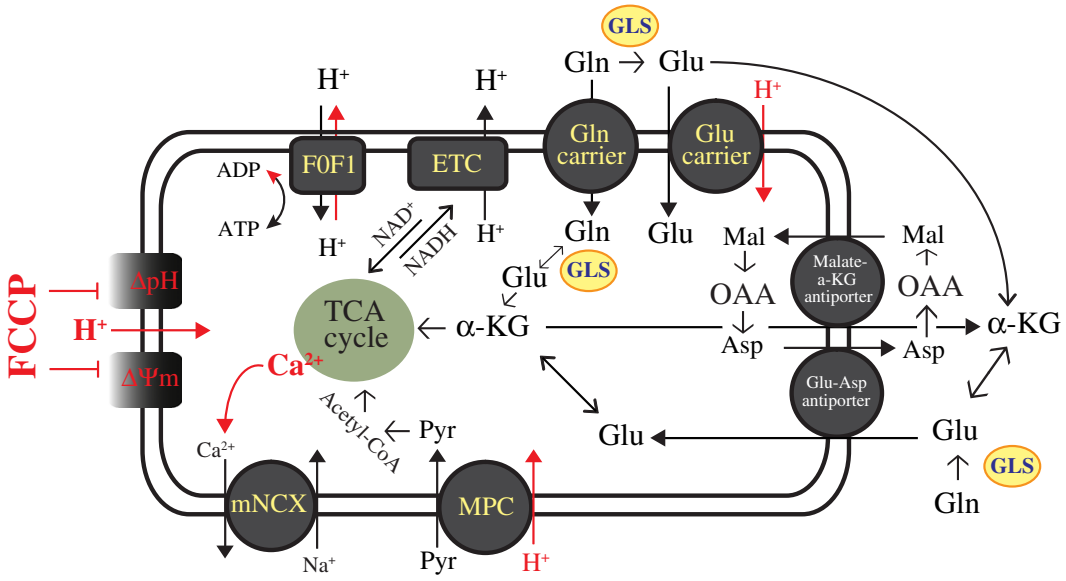

Fig. 6. Proposed effects of FCCP on the transport of the metabolic substrates across the mitochondrial membrane and efficiency of their utilisation (a simplified scheme). Gln is transported into the mitochondria via a Gln carrier, or is converted by glutaminase (GLS) into Glu which enters the mitochondria either through Mal–Asp shuttle or Glu carrier, to give rise to α-KG in the matrix. Pyr is transported into the matrix by the mitochondrial Pyr carrier (MPC). 1 μM FCCP dissipates ΔpH and depolarises ΔΨm, thus decreasing the rates of Gln and Glu delivery to the mitochondria.

induced ROS-dependent apoptosis in cancer cells, since Gln is one of the precursors of an antioxidant GSH [70]. FCCP has been shown to decrease the level of GSH and activity of the mitochondrial superoxide dismutase in a number of cancer cell lines, causing an increase in ROS levels after 48 h of treatment, which was associated with cell death [71,72].

A decrease in NAD(P)H levels and ROS production (at early stages of FCCP treatment) [73,74], changes in ATP and Ca^{2+} turnover—all can mutually modulate activity of the major pathways involved in cell metabolism and energy production. Upon FCCP treatment we found significant decrease in the phosphorylation of Erk p44/p42 (Thr202/Tyr204), Akt (Ser473), AMPKα (Thr-172) and mTOR (Ser2448) in all cells fed with Glc in combinations with Gln and Pyr (Fig. 3D). A decrease in Erk and Akt phosphorylation was more pronounced in the cells supplied with both Glc and Gln, capable of producing a strong respiratory response. We cannot explain these effects, however most probably they are ATP-independent, because ATP levels in the presence of Glc were not affected by uncoupling. On the other hand, an increase in NAD(P)/NAD(P)H ratio and cytosolic Ca^{2+}, as well as a decrease in ROS production may largely affect phosphorylation of these proteins. Surprisingly, in cells supplied with Gal/Gln/Pyr we observed a decrease in AMPKα phosphorylation, which is known to increase with an elevation of AMP/ATP ratio, ADP and ROS levels [75,76]. We believe that, since in these cells FCCP reduced both ATP and ROS, a decrease in the latter might have compensated for a decrease in the former. In contrast, Erk and particularly Akt phosphorylation in the medium containing Gal/Gln/Pyr was increased. We propose that such a strong elevation of phospho-Akt suggests an attempt to increase glycolysis (though not feasible without Glc), which is regulated by Akt in cancer cells [77]. In the cells supplied with Gal/Gln and treated with FCCP, protein phosphorylation was barely detectable, which can be related to a massive increase of apoptosis (Fig. 1D). Interplay between metabolic substrates, activity of the major pathways and respiration upon uncoupling require further investigation.

Overall, our results demonstrate that for significant response to uncoupling to be achieved both Gln and Pyr (including Pyr produced from Glc) are required, as FCCP can strongly decrease influx of these metabolites into the mitochondrial matrix.

In agreement with the concept of 'shared' contribution of the OxPhos and glycolysis in the maintenance of cellular ATP pool, L-ECA analysis demonstrated that glycolytic activity was inversely related to OCR. Thus, the rate of lactate extrusion from the cells supplied with Glc/Gln/Pyr was the lowest, since OxPhos in these cells was the highest among the cells grown in the presence of Glc (Fig. 2). Upon uncoupling, the most prominent increase in glycolysis is observed in the cells supplied with Gln, which may be associated with an increased Glc transport in these cells (through MondoA pathway). On the other hand, these cells exhibited strong sustained response to FCCP, which may require additional ATP production through glycolysis. However, this is doubtful, because the cells deprived of Glc with extremely low ATP levels are able to produce even stronger respiratory responses to uncoupling (Figs. 1, 2).

Although in the presence of Gln or Gln/Gal respiration drops upon uncoupling, Gln metabolism is the major contributor to the response to FCCP in both cancer cell lines (PC12 and HCT116). This was confirmed in the experiments with BPTES, which downregulates glutaminolysis through specific inhibition of GLS1. Interestingly, in the presence of BPTES 'resting' respiration was only slightly decreased, while the response to FCCP was almost completely abolished. This suggests that residual GLS1 activity (~20% of the maximal level [24]) is only sufficient to maintain resting but not the maximal respiration rates. Moreover, respiration in PC12 cells supplied with Gln and treated with BPTES dropped below the resting levels upon uncoupling. Glycolytic activity in resting cells supplied by Glc/Pyr/Gln or Glc/Gln was elevated to maintain ATP levels upon GLS1 inhibition (Fig. 4, Table 3). Upon FCCP treatment, L-ECA increased only in the cells supplied with Glc/Gln/Pyr. This could be credited to increased glycolysis and exogenous Pyr resulting in overall increase in Pyr which is converted into lactate, thereby contributing to L-ECA rate.

The respiratory responses of HCT116 cells to uncoupling were similar to that of PC12, with a smaller effect seen when GLS1 was inhibited. The respiration decreased but not blunted like in PC12 cells. This could be due to relatively low sensitivity of HCT116 cells to BPTES treatment (compare Figs. 4A and 5A) due to high expression of GLS2 [78], a p53-inducible liver type glutaminase, which is resistant to BPTES [79].

Resting and uncoupled respiration of MEFs were also substrate-dependent. However, the responses to FCCP differed significantly from the two cancer lines. In the optimal media (Fig. 5), FCCP induced less sustained and pronounced increase in respiration, than in the cancer

cells. Although Gln remained very important for active respiration, the contribution of Glc and Pyr to the respiratory response was more substantial than in PC12 and HCT116 cells. Illustrating this phenomenon, the most pronounced decrease in O_2 was observed in the cells supplied with Glc/Pyr/Gln, similar to the response in PC12 and HCT116 cells supplied with Gal/Pyr/Gln (Figs. 1B, 5A). Highlighting the decreased contribution of glutaminolysis to the uncoupling response in these cells, MEFs supplied with Glc/Pyr produced positive response to FCCP (Fig. 5C). Finally, an inhibition of GLS1 caused only partial decrease in the response to uncoupling, indicating that MEFs were capable of generating a Gln-independent response to FCCP stimulation. However, further comparative analysis of apoptosis, activity of the major metabolic and signalling pathways upon mitochondrial uncoupling in cancer and non-cancer cells is required.

Taken together, these data demonstrate that respiratory response to FCCP and O_2 levels in uncoupled cells are strongly modulated by the availability of metabolic substrates. Although difficult to translate directly to in vivo models, the conditions used in this work resemble a number of common (patho)physiological conditions including: i) reduced supply of nutrients and O_2 during ischemia/stroke [80]; ii) age-related decrease in glutamine synthase activity in astrocytes which supply neurons with Gln [81]; iii) hypoglycaemia in the patients with liver carcinoma [82] and diabetes mellitus [83]; and iv) cancer-associated changes in expression levels of the mitochondrial uncoupling proteins [84]. Cancer cells have altered metabolism and mitochondrial function [18], and pharmacological uncoupling has particular relevance to the development of drugs for cancer therapy, related to mitochondrial damage [71,72]. Here we show that cancer cells can be distinguished by specific response to FCCP, which strongly depends on the supply and utilisation of Gln and Glc. Such a specificity of the response demonstrates a potential application of mitochondrial uncoupling for substrate-dependent impairment of cancer metabolism.

Supplementary data to this article can be found online at http://dx.doi.org/10.1016/j.bbabio.2013.07.008.

Acknowledgements

Authors would like to thank Dr. Takashi Tsukamoto for generously providing us with BPTES and Ms. Sarah Cronin for technical contribution to the experiments with MEFs. This work was supported by SFI (grant no. 07/IN.1/B1804) and EU FP7 Marie Curie ITN Program “Chebana”, grant agreement no. 264772.

References

[1] M. Brand, The efficiency and plasticity of mitochondrial energy transduction, Biochem. Soc. Trans. 33 (2005) 897–904.
[2] B. Kadenbach, Intrinsic and extrinsic uncoupling of oxidative phosphorylation, Biochim. Biophys. Acta. Bioenerg. 1604 (2003) 77–94.
[3] H. Terada, Uncouplers of oxidative phosphorylation, Environ. Heal. Perspect. 87 (1990) 213.
[4] P. Heytler, W. Prichard, A new class of uncoupling agents—carbonyl cyanide phenylhydrazones, Biochem. Biophys. Res. Commun. 7 (1962) 272.
[5] R. Benz, S. McLaughlin, The molecular mechanism of action of the proton ionophore FCCP (carbonylcyanide p-trifluoromethoxyphenylhydrazone), Biophys. J. 41 (1983) 381–398.
[6] D.G. Nicholls, The influence of respiration and ATP hydrolysis on the proton-electrochemical gradient across the inner membrane of rat-liver mitochondria as determined by ion distribution, Eur. J. Biochem. 50 (1974) 305–315.
[7] I.D. Scott, D.G. Nicholls, Energy transduction in intact synaptosomes. Influence of plasma-membrane depolarization on the respiration and membrane potential of internal mitochondria determined in situ, Biochem. J. 186 (1980) 21–33.
[8] M.D. Brand, D.G. Nicholls, Assessing mitochondrial dysfunction in cells, Biochem. J. 435 (2011) 297–312.
[9] P.C. Hinkle, P/O ratios of mitochondrial oxidative phosphorylation, Biochim. Biophys. Acta 1706 (2005) 1–11.
[10] P. Weisová, U. Anilkumar, C. Ryan, C.G. Concannon, J.H.M. Prehn, M.W. Ward, ‘Mild mitochondrial uncoupling’ induced protection against glutamate excitotoxicity in primary neurons requires AMPK activity, Biochim. Biophys. Acta. Bioenerg. (2012).
[11] M.G. Vander Heiden, L.C. Cantley, C.B. Thompson, Understanding the Warburg effect: the metabolic requirements of cell proliferation, Sci. Signal. 324 (2009) 1029.
[12] T. McFate, A. Mohyeldin, H. Lu, J. Thakar, J. Henriques, N.D. Halim, H. Wu, M.J. Schell, T.M. Tsang, O. Teahan, S. Zhou, J.A. Califano, N.H. Jeoung, R.A. Harris, A. Verma, Pyruvate dehydrogenase complex activity controls metabolic and malignant phenotype in cancer cells, J. Biol. Chem. 283 (2008) 22700–22708.
[13] H.R. Christofk, M.G. Vander Heiden, M.H. Harris, A. Ramanathan, R.E. Gerszten, R. Wei, M.D. Fleming, S.L. Schreiber, L.C. Cantley, The M2 splice isoform of pyruvate kinase is important for cancer metabolism and tumour growth, Nature 452 (2008) 230–233.
[14] T. Hitosugi, S. Kang, M.G. Vander Heiden, T.W. Chung, S. Elf, K. Lythgoe, S. Dong, S. Lonial, X. Wang, G.Z. Chen, J. Xie, T.L. Gu, R.D. Polakiewicz, J.L. Roesel, T.J. Boggon, F.R. Khuri, D.G. Gilliland, L.C. Cantley, J. Kaufman, J. Chen, Tyrosine phosphorylation inhibits PKM2 to promote the Warburg effect and tumor growth, Sci. Signal. 2 (2009) ra73.
[15] P.S. Ward, C.B. Thompson, Metabolic reprogramming: a cancer hallmark even warburg did not anticipate, Cancer Cell 21 (2012) 297–308.
[16] D.R. Wise, R.J. DeBerardinis, A. Mancuso, N. Sayed, X.Y. Zhang, H.K. Pfeiffer, I. Nissim, E. Daikhin, M. Yudkoff, S.B. McMahon, C.B. Thompson, Myc regulates a transcriptional program that stimulates mitochondrial glutaminolysis and leads to glutamine addiction, Proc. Natl. Acad. Sci. U. S. A. 105 (2008) 18782–18787.
[17] D. Anastasiou, L.C. Cantley, Breathless cancer cells get fat on glutamine, Cell Res. 22 (2012) 443–446.
[18] R.A. Cairns, I.S. Harris, T.W. Mak, Regulation of cancer cell metabolism, Nat. Rev. Cancer 11 (2011) 85–95.
[19] D.R. Wise, C.B. Thompson, Glutamine addiction: a new therapeutic target in cancer, Trends Biochem. Sci. 35 (2010) 427–433.
[20] L.J. Reitzer, B.M. Wice, D. Kennell, Evidence that glutamine, not sugar, is the major energy source for cultured HeLa cells, J. Biol. Chem. 254 (1979) 2669–2676.
[21] J. Hynes, S. Floyd, A.E. Soini, R. O'Connor, D.B. Papkovsky, Fluorescence-based cell viability screening assays using water-soluble oxygen probes, J. Biomol. Screen. 8 (2003) 264–272.
[22] A. Fercher, S.M. Borisov, A.V. Zhdanov, I. Klimant, D.B. Papkovsky, Intracellular O2 sensing probe based on cell-penetrating phosphorescent nanoparticles, ACS Nano 5 (2011) 5499–5508.
[23] J. Hynes, T.C. O'Riordan, A.V. Zhdanov, G. Uray, Y. Will, D.B. Papkovsky, In vitro analysis of cell metabolism using a long-decay pH-sensitive lanthanide probe and extracellular acidification assay, Anal. Biochem. 390 (2009) 21–28.
[24] M.M. Robinson, S.J. McBryant, T. Tsukamoto, C. Rojas, D.V. Ferraris, S.K. Hamilton, J.C. Hansen, N.P. Curthoys, Novel mechanism of inhibition of rat kidney-type glutaminase by bis-2-(5-phenylacetamido-1,2,4-thiadiazol-2-yl)ethyl sulfide (BPTES), Biochem. J. 406 (2007) 407–414.
[25] D.G. Nicholls, Simultaneous monitoring of ionophore- and inhibitor-mediated plasma and mitochondrial membrane potential changes in cultured neurons, J. Biol. Chem. 281 (2006) 14864–14874.
[26] A.V. Zhdanov, M.W. Ward, C.T. Taylor, E.A. Souslova, D.M. Chudakov, J.H. Prehn, D.B. Papkovsky, Extracellular calcium depletion transiently elevates oxygen consumption in neurosecretory PC12 cells through activation of mitochondrial Na(+)/Ca(2+) exchange, Biochim. Biophys. Acta 1797 (2010) 1627–1637.
[27] R.I. Dmitriev, D.B. Papkovsky, Optical probes and techniques for O2 measurement in live cells and tissue, Cell Mol. Life Sci. 69 (2012) 2025–2039.
[28] D.B. Papkovsky, R.I. Dmitriev, Biological detection by optical oxygen sensing, Chem. Soc. Rev. (2013).
[29] A.V. Zhdanov, C. Favre, L. O'Flaherty, J. Adam, R. O'Connor, P.J. Pollard, D.B. Papkovsky, Comparative bioenergetic assessment of transformed cells using a cell energy budget platform, Integr. Biol. (Camb) 3 (2011) 1135–1142.
[30] A.V. Zhdanov, V.I. Ogurtsov, C.T. Taylor, D.B. Papkovsky, Monitoring of cell oxygenation and responses to metabolic stimulation by intracellular oxygen sensing technique, Integr. Biol. (Camb) 2 (2010) 443–451.
[31] Y. Will, J. Hynes, V.I. Ogurtsov, D.B. Papkovsky, Analysis of mitochondrial function using phosphorescent oxygen-sensitive probes, Nat. Protoc. 1 (2007) 2563–2572.
[32] C. Favre, A. Zhdanov, M. Leahy, D. Papkovsky, R. O'Connor, Mitochondrial pyrimidine nucleotide carrier (PNC1) regulates mitochondrial biogenesis and the invasive phenotype of cancer cells, Oncogene 29 (2010) 3964–3976.
[33] V. Choubey, D. Safiulina, A. Vaarmann, M. Cagalinec, P. Wareski, M. Kuum, A. Zharkovsky, A. Kaasik, Mutant A53T α-synuclein induces neuronal death by increasing mitochondrial autophagy, J. Biol. Chem. 286 (2011) 10814–10824.
[34] A.V. Zhdanov, R.I. Dmitriev, A.V. Golubeva, S.A. Gavrilova, D.B. Papkovsky, Chronic hypoxia leads to a glycolytic phenotype and suppressed HIF-2 signaling in PC12 cells, Biochim. Biophys. Acta 1830 (2013) 3553–3569.
[35] F. Farabegoli, M. Vettraino, M. Manerba, L. Fiume, M. Roberti, G. Di Stefano, Galloflavin, a new lactate dehydrogenase inhibitor, induces the death of human breast cancer cells with different glycolytic attitude by affecting distinct signaling pathways, Eur J Pharm Sci. 47 (2012) 729–738.
[36] G. Jasionek, A. Zhdanov, J. Davenport, L.k. Bláha, D.B. Papkovsky, Mitochondrial toxicity of microcystin-LR on cultured cells: application to the analysis of contaminated water samples, Environ. Sci. Technol. 44 (2010) 2535–2541.
[37] M. Porceddu, N. Buron, C. Roussel, G. Labbe, B. Fromenty, A. Borgne-Sanchez, Prediction of liver injury induced by chemicals in human with a multiparametric assay on isolated mouse liver mitochondria, Toxicol. Sci. 129 (2012) 332–345.
[38] K. Schouest, A. Zitova, C. Spillane, D.B. Papkovsky, Toxicological assessment of chemicals using *Caenorhabditis elegans* and optical oxygen respirometry, Environ. Toxicol. Chem. 28 (2009) 791–799.
[39] A. Zitova, F.C. O'Mahony, M. Cross, J. Davenport, D.B. Papkovsky, Toxicological profiling of chemical and environmental samples using panels of test organisms and optical oxygen respirometry, Environ. Toxicol. 24 (2009) 116–127.
[40] T.C. O'Riordan, A.V. Zhdanov, G.V. Ponomarev, D.B. Papkovsky, Analysis of intracellular oxygen and metabolic responses of mammalian cells by time-resolved fluorometry, Anal. Chem. 79 (2007) 9414–9419.

[41] T.C. O'Riordan, K. Fitzgerald, G.V. Ponomarev, J. Mackrill, J. Hynes, C. Taylor, D.B. Papkovsky, Sensing intracellular oxygen using near-infrared phosphorescent probes and live-cell fluorescence imaging, Am. J. Physiol. Regul. Integr. Comp. Physiol. 292 (2007) R1613–R1620.
[42] A.V. Zhdanov, M.W. Ward, J.H. Prehn, D.B. Papkovsky, Dynamics of intracellular oxygen in PC12 Cells upon stimulation of neurotransmission, J. Biol. Chem. 283 (2008) 5650–5661.
[43] K.A. O'Hagan, S. Cocchiglia, A.V. Zhdanov, M.M. Tambuwala, E.P. Cummins, M. Monfared, T.A. Agbor, J.F. Garvey, D.B. Papkovsky, C.T. Taylor, PGC-1α is coupled to HIF-1α-dependent gene expression by increasing mitochondrial oxygen consumption in skeletal muscle cells, Proc. Natl. Acad. Sci. 106 (2009) 2188–2193.
[44] R.I. Dmitriev, H.M. Ropiak, D.V. Yashunsky, G.V. Ponomarev, A.V. Zhdanov, D.B. Papkovsky, Bactenecin 7 peptide fragment as a tool for intracellular delivery of a phosphorescent oxygen sensor, FEBS J. 277 (2010) 4651–4661.
[45] R.I. Dmitriev, A.V. Zhdanov, G.V. Ponomarev, D.V. Yashunski, D.B. Papkovsky, Intracellular oxygen-sensitive phosphorescent probes based on cell-penetrating peptides, Anal. Biochem. 398 (2010) 24–33.
[46] R.I. Dmitriev, H.M. Ropiak, G.V. Ponomarev, D.V. Yashunsky, D.B. Papkovsky, Cell-penetrating conjugates of coproporphyrins with oligoarginine peptides: rational design and application for sensing intracellular O2, Bioconjug. Chem. 22 (2011) 2507–2518.
[47] A.V. Kondrashina, R.I. Dmitriev, S.M. Borisov, I. Klimant, I. O'Brien, Y.M. Nolan, A.V. Zhdanov, D.B. Papkovsky, A phosphorescent nanoparticle-based probe for sensing and imaging of (intra) cellular oxygen in multiple detection modalities, Adv. Funct. Mater. 22 (2012) 4931–4939.
[48] A.V. Zhdanov, R.I. Dmitriev, D.B. Papkovsky, Bafilomycin A1 activates HIF-dependent signalling in human colon cancer cells via mitochondrial uncoupling, Biosci. Rep. 32 (2012) 587–595.
[49] A.V. Zhdanov, R.I. Dmitriev, D.B. Papkovsky, Bafilomycin A1 activates respiration of neuronal cells via uncoupling associated with flickering depolarization of mitochondria, Cell Mol. Life Sci. 68 (2011) 903–917.
[50] C.M. O'Driscoll, A.M. Gorman, Hypoxia induces neurite outgrowth in PC12 cells that is mediated through adenosine A2A receptors, Neuroscience 131 (2005) 321–329.
[51] S.C. Taylor, C. Peers, Hypoxia evokes catecholamine secretion from rat pheochromocytoma PC-12 cells, Biochem. Biophys. Res. Commun. 248 (1998) 13–17.
[52] L.A. Greene, A.S. Tischler, Establishment of a noradrenergic clonal line of rat adrenal pheochromocytoma cells which respond to nerve growth factor, Proc. Natl. Acad. Sci. U. S. A. 73 (1976) 2424–2428.
[53] Y.A. Lazebnik, S.H. Kaufmann, S. Desnoyers, G.G. Poirier, W.C. Earnshaw, Cleavage of poly(ADP-ribose) polymerase by a proteinase with properties like ICE, Nature 371 (1994) 346–347.
[54] N. Mizushima, T. Yoshimori, How to interpret LC3 immunoblotting, Autophagy 3 (2007) 542–545.
[55] J. Zhu, M. Abate, P.W. Rice, C.N. Cole, The ability of simian virus 40 large T antigen to immortalize primary mouse embryo fibroblasts cosegregates with its ability to bind to p53, J. Virol. 65 (1991) 6872–6880.
[56] D.L. Poulin, J.A. DeCaprio, Is there a role for SV40 in human cancer? J. Clin. Oncol. 24 (2006) 4356–4365.
[57] J. Albrecht, M. Dolińska, W. Hilgier, A. Lipkowski, J. Nowacki, Modulation of glutamine uptake and phosphate-activated glutaminase activity in rat brain mitochondria by amino acids and their synthetic analogues, Neurochem. Int. 36 (2000) 341–347.
[58] B. Roberg, I.A. Torgner, E. Kvamme, Glutamine transport in rat brain synaptic and non-synaptic mitochondria, Neurochem. Res. 24 (1999) 383–390.
[59] F. Frigerio, M. Casimir, S. Carobbio, P. Maechler, Tissue specificity of mitochondrial glutamate pathways and the control of metabolic homeostasis, Biochim. Biophys. Acta. Bioenerg. 1777 (2008) 965–972.
[60] K.F. LaNoue, M.E. Tischler, Electrogenic characteristics of the mitochondrial glutamate-aspartate antiporter, J. Biol. Chem. 249 (1974) 7522–7528.
[61] G. Fiermonte, L. Palmieri, S. Todisco, G. Agrimi, F. Palmieri, J.E. Walker, Identification of the mitochondrial glutamate transporter, J. Biol. Chem. 277 (2002) 19289–19294.
[62] D.K. Bricker, E.B. Taylor, J.C. Schell, T. Orsak, A. Boutron, Y.-C. Chen, J.E. Cox, C.M. Cardon, J.G. Van Vranken, N. Dephoure, A mitochondrial pyruvate carrier required for pyruvate uptake in yeast, Drosophila Hum. Sci. 337 (2012) 96–100.
[63] S. Herzig, E. Raemy, S. Montessuit, J.-L. Veuthey, N. Zamboni, B. Westermann, E.R. Kunji, J.-C. Martinou, Identification and functional expression of the mitochondrial pyruvate carrier, Science 337 (2012) 93–96.
[64] M.R. Kaadige, R.E. Looper, S. Kamalanaadhan, D.E. Ayer, Glutamine-dependent anapleurosis dictates glucose uptake and cell growth by regulating MondoA transcriptional activity, Proc. Natl. Acad. Sci. U. S. A. 106 (2009) 14878–14883.
[65] C.W. Peterson, D.E. Ayer, An extended Myc network contributes to glucose homeostasis in cancer and diabetes, Front. Biosci. 17 (2011) 2206–2223.
[66] C.W. Peterson, C.A. Stoltzman, M.P. Sighinolfi, K.S. Han, D.E. Ayer, Glucose controls nuclear accumulation, promoter binding, and transcriptional activity of the MondoA-Mlx heterodimer, Mol. Cell. Biol. 30 (2010) 2887–2895.
[67] R.M. Denton, Regulation of mitochondrial dehydrogenases by calcium ions, Biochim. Biophys. Acta 1787 (2009) 1309–1316.
[68] K.B. Wallace, A.A. Starkov, Mitochondrial targets of drug toxicity, Annu. Rev. Pharmacol. Toxicol. 40 (2000) 353–388.
[69] S. Kuruvilla, C.W. Qualls Jr., R.D. Tyler, S.M. Witherspoon, G.R. Benavides, L.W. Yoon, K. Dold, R.H. Brown, S. Sangiah, K.T. Morgan, Effects of minimally toxic levels of carbonyl cyanide P-(trifluoromethoxy) phenylhydrazone (FCCP), elucidated through differential gene expression with biochemical and morphological correlations, Toxicol. Sci. 73 (2003) 348–361.
[70] G. Wu, Y.-Z. Fang, S. Yang, J.R. Lupton, N.D. Turner, Glutathione metabolism and its implications for health, J. Nutr. 134 (2004) 489–492.
[71] Y.H. Han, W.H. Park, Intracellular glutathione levels are involved in carbonyl cyanide p-(trifluoromethoxy) phenylhydrazone-induced apoptosis in As4.1 juxtaglomerular cells, Int. J. Mol. Med. 27 (2011) 575–581.
[72] Y.H. Han, S.H. Kim, S.Z. Kim, W.H. Park, Carbonyl cyanide p-(trifluoromethoxy) phenylhydrazone (FCCP) as an O2(*-) generator induces apoptosis via the depletion of intracellular GSH contents in Calu-6 cells, Lung Cancer 63 (2009) 201–209.
[73] A.A. Starkov, G. Fiskum, Regulation of brain mitochondrial H2O2 production by membrane potential and NAD(P)H redox state, J. Neurochem. 86 (2003) 1101–1107.
[74] J.P. Brennan, R.G. Berry, M. Baghai, M.R. Duchen, M.J. Shattock, FCCP is cardioprotective at concentrations that cause mitochondrial oxidation without detectable depolarisation, Cardiovasc. Res. 72 (2006) 322–330.
[75] P.T. Mungai, G.B. Waypa, A. Jairaman, M. Prakriya, D. Dokic, M.K. Ball, P.T. Schumacker, Hypoxia triggers AMPK activation through reactive oxygen species-mediated activation of calcium release-activated calcium channels, Mol. Cell. Biol. 31 (2011) 3531–3545.
[76] S.A. Hawley, M. Davison, A. Woods, S.P. Davies, R.K. Beri, D. Carling, D.G. Hardie, Characterization of the AMP-activated protein kinase kinase from rat liver and identification of threonine 172 as the major site at which it phosphorylates AMP-activated protein kinase, J. Biol. Chem. 271 (1996) 27879–27887.
[77] R.L. Elstrom, D.E. Bauer, M. Buzzai, R. Karnauskas, M.H. Harris, D.R. Plas, H. Zhuang, R.M. Cinalli, A. Alavi, C.M. Rudin, C.B. Thompson, Akt stimulates aerobic glycolysis in cancer cells, Cancer Res. 64 (2004) 3892–3899.
[78] S. Suzuki, T. Tanaka, M.V. Poyurovsky, H. Nagano, T. Mayama, S. Ohkubo, M. Lokshin, H. Hosokawa, T. Nakayama, Y. Suzuki, Phosphate-activated glutaminase (GLS2), a p53-inducible regulator of glutamine metabolism and reactive oxygen species, Sci. Signal. 107 (2010) 7461.
[79] B. DeLaBarre, S. Gross, C. Fang, Y. Gao, A. Jha, F. Jiang, J. Song, J.W. Wei, J.B. Hurov, Full-length human glutaminase in complex with an allosteric inhibitor, Biochemistry 50 (2011) 10764–10770.
[80] N.R. Sims, H. Muyderman, Mitochondria, oxidative metabolism and cell death in stroke, Biochim. Biophys. Acta 1802 (2010) 80–91.
[81] M.L. Steele, S.R. Robinson, Reactive astrocytes give neurons less support: implications for Alzheimer's disease, Neurobiol. Aging 33 (2012), (423. e421-423. e).
[82] H.B. El-Serag, J.A. Marrero, L. Rudolph, K.R. Reddy, Diagnosis and treatment of hepatocellular carcinoma, Gastroenterology 134 (2008) 1752–1763.
[83] P.E. Cryer, S.N. Davis, H. Shamoon, Hypoglycemia in diabetes, Diabetes Care 26 (2003) 1902–1912.
[84] V. Azzu, M. Jastroch, A.S. Divakaruni, M.D. Brand, The regulation and turnover of mitochondrial uncoupling proteins, Biochim. Biophys. Acta. Bioenerg. 1797 (2010) 785–791.